

Modeling of a Non-Isothermal Fixed Bed Reactor: 1D Model for Hydrogen Production by Steam Methane Reforming

Bellal Mohamed Nazim*, Saouli Ouacil, Masbah Aflah, Drede Abdlehamid

Laboratoire de Génie des Procédés pour le Développement Durable et les Produits de Santé (GPDDPS), Département Génie des Procédés, Ecole Nationale Polytechnique de Constantine, Algeria.
nazimnazim2@gmail.com

A numerical study was conducted to assess the overall heat transfer coefficient for exterior/reactor convection energy transfer in a steady-state, one-dimensional, pseudo-homogeneous, non-isothermal model of hydrogen production by steam methane reforming (SMR). The study primarily focuses on comparing a catalytic packed-bed reactor (PBR) with a Pd-based catalytic membrane reactor (MR). A selectively permeable Pd-based membrane is utilized to extract hydrogen from the reaction zone, promoting a shift in the thermodynamic equilibrium towards hydrogen production and facilitating higher methane conversion. The hydrogen is then transported away by a sweep gas, typically H₂O. The mathematical models were simulated using MATLAB. Additionally, the influence of key operating parameters was investigated using comprehensive reactor models.

1. Introduction

Hydrogen is gaining increasing significance due to its use in automobile and household fuel cells. The most common method of hydrogen production involves utilizing fossil fuels such as natural gas and coal, due to their high efficiency, low heating value, and cost-effectiveness. However, there is growing interest in using renewable feedstocks like biomass, biogas, and bioethanol. Literature contains studies on isothermal membrane reactors (Kuncharam and Dixon, 2020). However, considering the highly endothermic nature of the methane steam reforming process, investigations have been conducted on non-isothermal models (Daymo et al., 2024). Continuous heat supply is required to maintain an appropriate process temperature, typically achieved by hot gas flowing along the outer wall of the reactor.

Previous studies have adopted different assumptions for the overall heat transfer coefficient (U_{OR}). (Madia et al., 1999) assumed a constant U_{OR} of 817.2 kJ/(m²·h·K) across the reactor, irrespective of operating conditions. Similarly, (Wu et al., 2023) performed a numerical investigation of steam methane reforming in a packed bed reactor installed with Metal Foam with a fixed U_{OR} for each foam model, (Dong et al., 2019) performed an optimization analysis within the range of 241.56–946.8 kJ/(m²·h·K), while (Park et al., 2019) used a fixed value of 360 kJ/(m²·h·K). However, these approaches do not account for the dynamic variations in heat transfer influenced by fluid dynamics and varying operating conditions along the reactor length.

The objective of this study is to improve the accuracy of the steam methane reforming simulation by integrating a variable U_{OR} into a comparative numerical simulation of two reactor types: a packed-bed reactor (PBR) and a membrane reactor (MR) with co-current flow. By focusing on methane (CH₄) conversion, and the effects of multiple parameters such as inlet flow rate, steam to methane ratio, and the inlet temperature, this approach aims to enhance operational conditions using a non-isothermal model to account for temperature variations.

2. Mathematical Model

Reaction Kinetics

In general, steam methane reforming is modeled through three key global reactions: methane reforming reaction (Endothermic):



water-gas shift reaction (Exothermic):



Overall Reaction:



Since the reforming process is endothermic, thermal energy input is necessary to sustain the conversion of methane into hydrogen. These reactions are modeled using the Langmuir-Hinshelwood mechanism (Xu and Froment, 1989), with rate expressions as follows:

$$r_1 = \frac{k_1}{P_{\text{H}_2}^{2.5}} \cdot \left(P_{\text{CH}_4} \cdot P_{\text{H}_2\text{O}} - \frac{P_{\text{H}_2}^3 \cdot P_{\text{CO}}}{K_1} \right) / D^2 \quad (4)$$

$$r_2 = \frac{k_2}{P_{\text{H}_2}} \cdot \left(P_{\text{CO}} \cdot P_{\text{H}_2\text{O}} - \frac{P_{\text{H}_2} \cdot P_{\text{CO}_2}}{K_2} \right) / D^2 \quad (5)$$

$$r_3 = \frac{k_3}{P_{\text{H}_2}^{3.5}} \cdot \left(P_{\text{CH}_4} \cdot P_{\text{H}_2\text{O}}^2 - \frac{P_{\text{H}_2}^4 \cdot P_{\text{CO}_2}}{K_3} \right) / D^2 \quad (6)$$

Where:

$$D = 1 + K_{\text{CO}} P_{\text{CO}} + K_{\text{H}_2} P_{\text{H}_2} + K_{\text{CH}_4} P_{\text{CH}_4} + K_{\text{H}_2\text{O}} \frac{P_{\text{H}_2\text{O}}}{P_{\text{H}_2}} \quad (7)$$

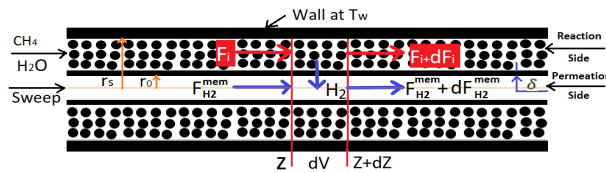
$$k_i = K_i = K_j = a \cdot \exp\left(-\frac{b}{T} + c\right) \quad (8)$$

The kinetic parameters are presented in Table 1, knowing that $K_3 = K_1 \cdot K_2$

Table 1: Kinetic variables (Xu and Froment, 1989; Saw et al., 2016)

variable	k_1	k_2	k_3	K_1	K_2	K_{CH_4}	$K_{\text{H}_2\text{O}}$	K_{CO}	K_{H_2}
a	$9.49 \cdot 10^{16}$	$4.39 \cdot 10^4$	$2.29 \cdot 10^{16}$	10,266.76	1	$6.65 \cdot 10^{-6}$	$1.77 \cdot 10^3$	$6.12 \cdot 10^{-11}$	$8.23 \cdot 10^{-7}$
b	28,879	8,074.3	29,336	26,830	4,400	4,604.28	10,666.35	9,971.13	8,497.71
c	0	0	0	30.11	-4.063	0	0	0	0

To represent the reactor design, a one-dimensional (1D) configuration was employed similar to the catalytic membrane reactor (MR) setups in previous studies (Iulianelli et al., 2016; Wu et al., 2020). As illustrated in Figure 1, the MR consists of a tubular permeation zone (fed with sweep gas in a co-current mode) and a reaction zone filled with catalyst particles, separated by a membrane.



Input + Generation = Output

$$F_i + \rho_c(\sum \eta_i r_j) dV = F_i + dF_i, \text{ where } dV = A_c \cdot dz$$

$$A_c = \pi(r_s^2 - (r_0 + \delta)^2)$$

$$F_{\text{CH}_4} + \rho_c(\eta_1 r_1 + \eta_3 r_3) dV = F_{\text{CH}_4} + dF_{\text{CH}_4}$$

$$F_{\text{CO}_2} + \rho_c(\eta_2 r_2 + \eta_3 r_3) dV = F_{\text{CO}_2} + dF_{\text{CO}_2}$$

Figure 1: Schematic of catalytic membrane reactor (MR) in co-current mode.

The PBR is a tube packed with catalyst particles and heated through the wall. The model for MR consists of mass and energy balances and is based on the following simplifying assumptions:

- Steady state condition,
- All gas species follow the ideal gas law,
- Plug flow conditions apply to both retentate and permeate streams,
- The inlet temperature is the same as the wall temperature: $T_{\text{react},0} = T_{\text{perm},0} = T_w$.
- Pseudo-homogeneous catalyst bed,

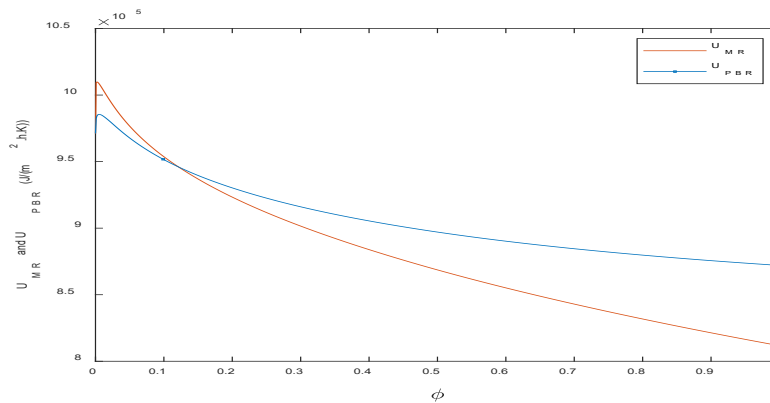
The differential equations governing mass and heat balances for both retentate zone and permeate zone are listed below, with Table 2 summarizing their form:

Table 2: differential equation used for the simulation (Wu et al., 2020).

Balance	zone	Equation
Mass balance	Reaction zone	$\frac{dX_{CH_4}}{d\phi} = \frac{\rho_c \cdot A_c \cdot L}{F^0_{CH_4}} \cdot (\eta_1 r_1 + \eta_3 r_3)$
		(9) $\frac{dX_{CO_2}}{d\phi} = \frac{\rho_c \cdot A_c \cdot L}{F^0_{CH_4}} \cdot (\eta_2 r_2 + \eta_3 r_3)$
		(10)
		$F_{CH_4} = F^0_{CH_4}, X_{CH_4} = 0 \text{ at } \phi=0.$
		(11) $Q_{pd} = 6.3227 \cdot 10^{-3} \cdot e^{\left(\frac{-15630}{RT}\right)}$
	Permeate zone	$\frac{dY_{H_2}}{d\phi} = \frac{Q_{pd} \cdot 2\pi \cdot (r_0 + \delta) \cdot L}{F^0_{CH_4} \cdot \delta \cdot 22.4} \cdot (P^{0.5}_{H_2 ret} - P^{0.5}_{H_2 per})$
		(12)
		$F_{H_2} = 0 \text{ at } \phi=0.$
Heat balance	Reaction zone	$\frac{dT_{react}}{d\phi} = \frac{\left(\sum_i (-\Delta H_{r,i}(T)) R_i \rho_c\right) \cdot A \cdot L - \sum_j C p_j^{react} \frac{dF_j}{d\phi} \cdot (T_{react} - T_{ref})}{\sum_j C p_j^{react} F_j}$
		$\frac{h_{memb} \cdot 2\pi \cdot (r_0 + \delta) \cdot L \cdot (T_{react} - T_{perm})}{\sum_j C p_j^{react} F_j} + \frac{U_{OR} \cdot 2\pi \cdot L \cdot (r_s + l) \cdot (T_W - T_{react})}{\sum_j C p_j^{react} F_j}$
		(13)
		$T = T_{react} - T_{Ref}$
		$T_{perm} = T_0 \text{ at } \phi = 0.$
	Permeate zone	$\frac{dT_{perm}}{d\phi} = \frac{C p_{H_2}^{react} \cdot F^0_{CH_4} \cdot \frac{dY_{H_2}}{d\phi} \cdot (\Delta T) + h_{memb} \cdot 2\pi \cdot (r_0 + \delta) \cdot L \cdot (\Delta T)}{C p_{sweep}^{perm} \cdot F_{sweep} + C p_{H_2}^{perm} \cdot F_{H_2}}$
		(14)

3. Results and discussion

The system of ordinary differential equations (ODEs), consisting of equations (9, 10, 12, 13, and 14), was solved numerically in MATLAB using the ode15s function. The steam methane reforming conditions are as follows: the system operates with initial reaction, permeation, and wall temperature of 500 °C. Methane is fed into the reactor at a rate of 1 kmol /h. The reactor is 1 m long, and the operating pressure is maintained at 1 bar. The reactor has an outer shell radius of 8.89 cm and an inner tube radius of 6.35 cm, with a catalyst density of 2100 kg/m³ and a bed porosity of 0.53. The permeate zone pressure is also set at 1 bar. The feed composition includes 24.99 % methane, 74.99 % water, 0.01% hydrogen, and no carbon monoxide or carbon dioxide. The membrane used has a radius of 2.54 cm and a thickness of 5·10⁻⁶ m, and operates with a sweep ratio of 20.

Figure 2 Variation of overall heat transfer coefficient in PBR and MR $P_T = 1$ bar.

The system's performance is evaluated based on key operating conditions, namely feed flow rate, temperature, steam/methane ratio. The most important parameters to assess are CH₄ conversion and temperature.

As shown in Figure 2, when the operating pressure is fixed at 1 bar, the overall heat transfer coefficient in the membrane reactor (U_{MR}) decreases at a faster rate compared to the overall heat transfer coefficient in the packed-bed reactor (U_{PBR}). Specifically, U_{MR} declined from 1,010 $\text{kJ}/(\text{m}^2\cdot\text{h}\cdot\text{K})$ to 813 $\text{kJ}/(\text{m}^2\cdot\text{h}\cdot\text{K})$, while U_{PBR} decreased from 984 $\text{kJ}/(\text{m}^2\cdot\text{h}\cdot\text{K})$ to 871 $\text{kJ}/(\text{m}^2\cdot\text{h}\cdot\text{K})$.

The overall heat transfer coefficient is influenced by the overall flow rate, which is related to the Reynolds number. In the PBR, the low permeation rate of hydrogen through the membrane, due to the low-pressure difference between the reaction zone and the permeation zone, prevents significant reversals in the reaction. As a result, it has a smaller impact on the Reynolds number and, consequently, on the overall heat transfer coefficient. Additionally, thermal conductivity decreases in both reactors due to the steam methane reforming (SMR) and water-gas shift (WGS) reactions, with CO_2 having the lowest thermal conductivity. As a consequence of this behavior, the temperature in the MR is lower than in the PBR as shown in Figure 3.

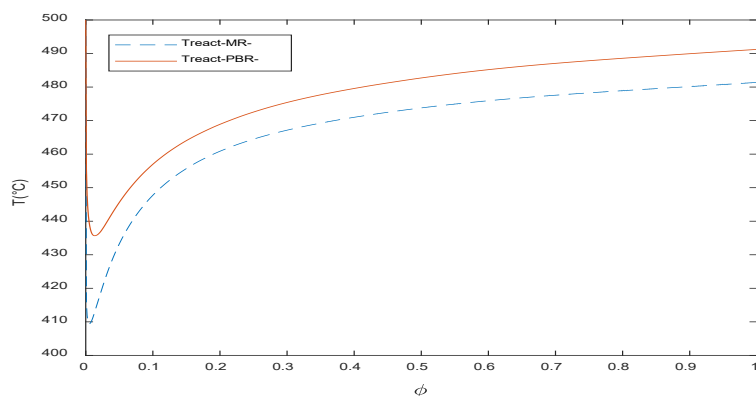


Figure 3. PBR and MR temperature profile ($T_{\text{react}0} = 500\text{ }^\circ\text{C}$).

Figure 3 shows the temperature profiles of the PBR and MR along the reactor length. The initial temperature decrease is due to the major consumption of reactants at the beginning of the reactor (up to $\phi = 0.02$). After this point, the heat generated by convection compensates for the temperature drop, causing an increase in temperature until thermal equilibrium is reached ($T_{\text{react}} = T_{\text{wall}}$).

Figure 4 shows the methane conversion for the PBR and MR along the reactor length.

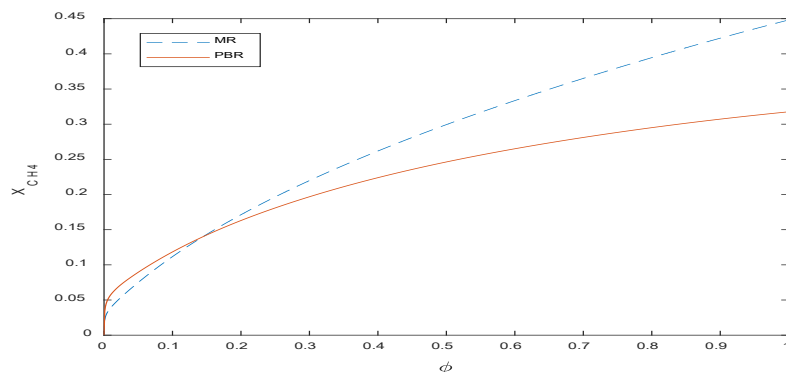


Figure 4: Methane conversion in PBR and MR.

It is clear that under the same conditions, the MR exhibits better performance than the PBR. In the membrane reactor, increasing the reaction pressure leads to a greater difference between the partial pressure of hydrogen on the reaction zone and the permeate zone. This increase in hydrogen permeation further enhances methane conversion.

MR showed better results compared to PBR so to investigate the mole fraction variation in the membrane reactor, the mole fraction percentages of the reactants and products are displayed in Figure 5 (co-current flow, steam/methane ratio $m = 3$).

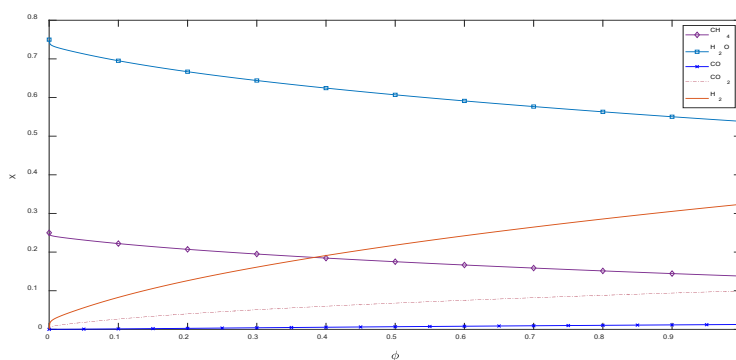


Figure 5: Molar fraction of each component ($F_{CH_4}=1$ kmol/h)

H_2 is the hydrogen flow that goes through the membrane. The inlet gas temperature was $500\text{ }^\circ\text{C}$ and the steam to methane ratio was 3 for this simulation. The methane mole fraction declined from 24.9 % to 13.8 %, while the hydrogen mole fraction increased from 0.01 % to 32.2 %. The CO and CO_2 mole fractions increased slightly. The increase in hydrogen mole fraction was consistently higher than the other products (CO and CO_2). The water mole fraction decreased from 74.99 % to 53.8 % due to the SMR reaction.

To improve methane conversion rates and increase hydrogen production, several parameters in the membrane reactor (MR) can be adjusted. Figure 6 highlights the effect of the steam-to-methane molar ratio m on methane conversion. This ratio, representing the balance between reactants, plays a significant role in driving the reforming reaction forward.

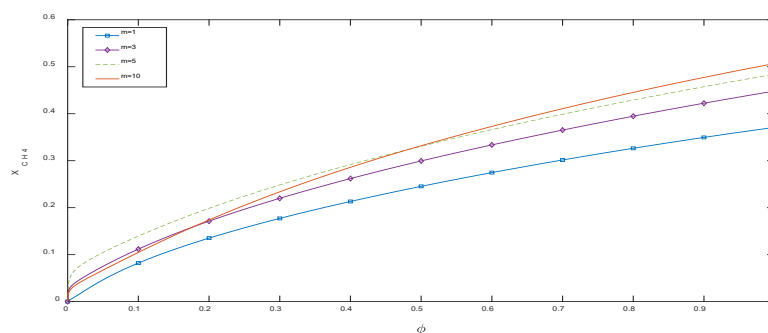


Figure 6: Steam-to-methane ratio effect on methane conversion ($F_{CH_4}=1$ kmol/h).

As shown in Figure 6, an increase in m enhances conversion, indicating that an excess of steam improves methane conversion. Beyond a ratio of $m = 3$, the rate of increase in conversion is reduced, suggesting that further increases in steam provide diminishing returns. This supports the initial selection of the chosen ratio.

The temperature plays a major role in the steam methane reforming reaction. Figure 7 shows that an increase in inlet temperature leads to a higher methane conversion.

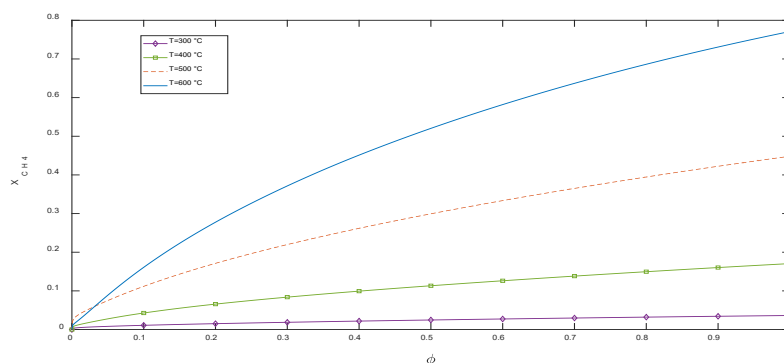


Figure 7: Inlet temperature effect on methane conversion ($F_{CH_4}=1$ kmol/h).

The Figure shows that higher inlet temperatures correlate strongly with increased conversion: at an inlet temperature of $T_{in}=600$ °C, the conversion reaches its highest level, whereas at $T_{in}=300$ °C, the conversion is minimal.

4. Conclusions

This study has demonstrated that the assimilation of a variable overall heat transfer coefficient (U_{OR}) in a non-isothermal model simulation of steam methane reforming (SMR) improves the predictive accuracy of the simulation for both packed-bed reactors (PBR) and membrane reactors (MR)

Results show that membrane reactors outperform PBRs by reaching a higher methane conversion under similar operating conditions. Key parameters, including inlet temperature, methane flow rate, and the steam-to-methane ratio, have significant effects on conversion efficiency. The minimum reactor temperature must be at least 500 °C or higher to achieve a decent conversion rate with an H_2O/CH_4 ratio of 3 and provides diminishing returns beyond this ratio. The H_2 production rate can be improved by increasing the temperature. For methane conversion, the inlet temperature has a positive effect, while the methane flow rate has a negative effect; their interaction, however, has a positive effect.

Nomenclature

PBR – Packed Bed Reactor	k_1, k_2, k_3 – rate coefficients, $kmol \cdot kPa^{0.5}/(kg \cdot h)$, $kmol \cdot kPa^{1/2}/(kg \cdot h)$, $kmol \cdot kPa^{0.5}/(kg \cdot h)$
MR – Membrane reactor	L – length of the reactor, m
r_i – kinetic rate of i^{th} reaction, $kmol/kg_{cat} \cdot h$	Cp_j – molar specific heat for j^{th} component, $J/mol \cdot K$
F_j^{in} – inlet j^{th} component molar flow rate, $kmol/h$	T_{react} – temperature of reaction zone, K
F_j – outlet j^{th} component molar flow rate, $kmol/h$	T_{perm} – temperature of permeation zone, K
P_j – partial pressure of j^{th} component, bar	h_{memb} – membrane heat transfer coefficient $J \cdot m^{-1} K^{-1}$
η_i – effectiveness factor of i^{th} reaction, -	K_j – absorption constant of component j -
A_c – cross section of the reactor m^2	K_1, K_2, K_3 – equilibrium constants,
δ – membrane thickness, μm	
ϕ – dimensionless length $\phi = \frac{z}{L}$, -	

References

- Daymo, E., Tonkovich, A., Hettel, M., Shirsath, A., 2024. 1D and 2D porous media fixed bed reactor simulations with DUO: Steam Methane Reforming (SMR) validation test. IOP Conf Ser Mater Sci Eng 1312, 012004. <https://doi.org/10.1088/1757-899x/1312/1/012004>
- Dong, X., Peng, L., Xiaoyou, Y., 2019. Process modeling, optimization, and heat integration of ethanol reforming process for syngas production with high H_2/CO ratio. Processes 7. <https://doi.org/10.3390/PR7120960>
- Iulianelli, A., Liguori, S., Wilcox, J., Basile, A., 2016. Advances on methane steam reforming to produce hydrogen through membrane reactors technology: A review. Catal Rev Sci Eng 58, 1–35. <https://doi.org/10.1080/01614940.2015.1099882>
- Kuncharam, B.V.R., Dixon, A.G., 2020. Multi-scale two-dimensional packed bed reactor model for industrial steam methane reforming. Fuel Processing Technology 200. <https://doi.org/10.1016/j.fuproc.2019.106314>
- Madia, G.S., Barbieri, G., Drioli, E., 1999. Theoretical and experimental analysis of methane steam reforming in a membrane reactor. Canadian Journal of Chemical Engineering 77, 698–706. <https://doi.org/10.1002/cjce.5450770411>
- Park, H.G., Han, S.Y., Jun, K.W., Woo, Y., Park, M.J., Kim, S.K., 2019. Bench-scale steam reforming of methane for hydrogen production. Catalysts 9, 1–14. <https://doi.org/10.3390/catal9070615>
- Saw, S.Z., Nandong, J., Ghosh, U.K., 2016. Comparative Study of Homogeneous and Heterogeneous Modelling of Water-Gas Shift Reaction with Macro-or Micro-kinetics, in: Procedia Engineering. Elsevier Ltd, pp. 949–956. <https://doi.org/10.1016/j.proeng.2016.06.467>
- Wu, H.C., Rui, Z., Lin, J.Y.S., 2020. Hydrogen production with carbon dioxide capture by dual-phase ceramic-carbonate membrane reactor via steam reforming of methane. J Memb Sci 598, 117780. <https://doi.org/10.1016/j.memsci.2019.117780>
- Wu, Z., Yang, J., Wang, Q., 2023. Numerical Investigation of Methane Steam Reforming in the Packed Bed Installed with Metal Foam. Chem Eng Trans 103, 67–72. <https://doi.org/10.3303/CET23103012>
- Xu, J., Froment, G.F., 1989. Methane steam reforming: II. Diffusional limitations and reactor simulation. AIChE Journal 35, 97–103. <https://doi.org/10.1002/aic.690350110>